Materials Today • Volume xxx, Number xx • xxxx 2017

ELSEVIER

SHORT COMMUNICATION (MID GREEN)

Aperiodicity is all you need: Aperiodic monotiles for high-performance composites

Jiyoung Jung [1], Ailin Chen [1], Grace X. Gu *

Department of Mechanical Engineering, University of California, Berkeley, CA 94720, USA

Developing mechanical materials with high stiffness, strength, and toughness has been a longstanding pursuit. Conventional engineering materials often experience a trade-off relationship between these properties, motivating researchers to explore composite structures to overcome these limitations. This study introduces a novel approach to composite design by employing aperiodic monotiles, shapes that cover surfaces without any translational symmetry. Using a combined computational and experimental approach, we study the fracture behavior of composites crafted with these monotiles and compare their performance against conventional honeycomb and square patterns. Remarkably, our aperiodic monotile-based composites exhibited superior Young's modulus, strength, and toughness in comparison to other designs under tensile loading conditions. In addition, the aperiodic monotile structures showed consistent mechanical performance with varying crack locations and directions, which implies reliable fracture resistance under complex loadings. This study suggests that leveraging the inherent disorder of aperiodic structures can usher in a new generation of robust and resilient materials.

Introduction

Composite materials, celebrated for their customizable mechanical properties, serve as lightweight structural components that are integral in the aerospace and biomedical sectors [1–5]. The strength of these materials lies in their composite nature – combining properties of different base materials allows the creation of a composite with a harmonious balance of multiple desired properties. This concept is beautifully exemplified in biological materials [6–11] such as nacre and wood, which generally outperform their engineering counterparts in mechanical performance, despite being composed of relatively weak constituents. Traditional engineering composites are often characterized by repeating unit cells, a feature that simplifies the design and manufacturing processes. However, such ordered structures can lead to catastrophic failure under critical loading. Meanwhile, biological materials often present disordered structures, where the unit cells vary spatially [12]. The extent to which this disorder plays a role in the improved mechanical performance of biological materials remains a topic of ongoing research.

The inherent benefits of materials with irregular or disordered microstructures have recently garnered scientific interest [13–16]. Characterized by heterogeneous microstructures, these structures could offer a fortified path for stress wave propagation, thereby increasing resilience under heavy loads [17–20]. Emerging research indicates that by amplifying this irregularity, the flaw tolerance of specific cellular frameworks can be enhanced [21]. Moreover, the microscopic intricacies of polycrystalline configurations, encompassing grain boundaries, precipitates, and phases, are perceived as prospective templates for engineering materials with enhanced toughness [22,23]. Current methodologies for creating these heterostructures involve techniques such as randomly moving nodes within regular lattice structures, constructing material foams, or stacking materials with different microstructures [18,24,25]. However, these methods introduce a

* Corresponding author.
E-mail address: Gu, G.X. (ggu@berkeley.edu)
[1] These authors contributed equally to this work.

 https://doi.org/10.1016/j.mattod.2023.12.015

Please cite this article in press as: J. Jung et al., Materials Today (2024), https://doi.org/10.1016/j.mattod.2023.12.015

layer of complexity to design and manufacturing, especially with challenges due to the imperfect assembly of differently oriented unit cells.

Addressing these challenges, our study presents the integration of aperiodic monotiles in composite designs. Aperiodic monotiles, as discovered in recent literature, have been shown to cover a surface entirely with intrinsic aperiodicity [26]. This makes them an ideal choice for creating disordered materials. The usage of aperiodic monotiles in composite design would facilitate tunable properties while maintaining excellent interface bonding. In this work, we explore a completely new family of architectures composed of aperiodic monotiles for creating composite materials. Specifically, we developed a numerical phase-field model to simulate the properties and crack propagation of composites consisting of aperiodic monotiles. Our models are validated with tensile experiments of additively manufactured specimens. The aperiodic monotile-based designs are benchmarked with periodic honeycomb-based design, which is one of the most widely used shapes in engineering applications due to its superior mechanical performance [27], and a traditional square-tile design. It is envisioned that these types of aperiodic designs could lead to the development of stronger and tougher composite materials compared to the conventional periodic designs.

Results and discussions

An aperiodic monotile is a shape that can cover a two-dimensional (2D) surface without any translational symmetry or a repeating pattern [26]. An example schematic of tiling using a 'hat' polykite aperiodic monotile [26] is shown in Fig. 1(a). Due to the characteristics of the hat monotile generated based on the hexagonal structure, the monotile can have six rotational angles and a flipped shape as shown in Fig. 1(b, c). These hat monotiles cover the infinite plane in an irregular manner, which enables limitless designs by translation and rotation of tiles. Here, we will introduce translation and rotation of the aperiodic monotile-based design along the reference tile, part of the infinite reference tile shown in Fig. 1(a) and study their influence on mechanical behavior.

Experiments are conducted to explore the mechanical performance of the aperiodic monotile-based composites. Mechanical tensile tests are conducted, with more details in the Methods section. In terms of material selection, two base constituents are utilized, one for the boundaries and another for the inner unit cell material. To evaluate the composites under realistic operational conditions, a defect is introduced, in the form of a notch, into the samples. This approach enables us to investigate the tolerance of these materials to such anomalies. For the fabrication process, Polyjet additive manufacturing (Stratasys Connex 3) is employed, utilizing digital photopolymer materials with a modulus range spanning over three orders of magnitude. Two digital photopolymer materials are used to achieve the required characteristics. In this case, TangoBlackPlus, the softer material, is used to form the boundaries, while VeroClear, the stiffer material, is used for the cores. The structures with stiff cores and soft boundaries, as in polycrystalline materials, are known to offer various benefits, including cracks detouring by confining cracks within the soft boundary, enhanced fatigue resistance, and efficient energy dissipation.

A specimen has dimensions of 50 mm by 125 mm by 3 mm with a notch of 20 % length of the specimen width (10 mm) as shown in Fig. 2(a). We prepared the specimens with different notch tip locations and volume fractions. For aperiodic monotile-based specimens, we have prepared three different specimens with a volume fraction of 80 % VeroClear and 20 % TangoBlackPlus where two specimens are subjected to a planar translation (denoted as AP80_T1 and AP80_T2) and a third specimen undergoes a rotation of 30 degrees (denoted as AP80_R1) along the infinite reference tile. Schematics of translation and rotation can be found in Fig. S1 in Supplementary Information. In the same manner, we also test three specimens with a volume fraction of 70 % VeroClear and 30 % TangoBlackPlus with translation and rotation (denoted as AP70_T1, AP70_T2, and AP70_R1). These designs are shown in Fig. 2(a). We note that infinitely many patterns can be generated by the translation or rotation of the tiling. As a benchmark, the honeycomb and square-tile structures which have a periodic pattern are considered as shown in Fig. 2(b, c). Two honeycomb-based specimens with different volume fractions are considered, denoted as HC80 and HC70, and their 30-degree rotated configurations are considered, denoted as HC80_R1 and HC70_R1. Square-tile specimens and their 45-degree rotated specimens are tested, denoted as SQ80, SQ80_R1, SQ70, and SQ70_R1.

Experimental stress–strain curve results for the various samples are presented in Fig. 3(a) and (b), where (a) and (b) are results for 80 % and 70 % volume fractions of VeroClear material, respectively. The shadows in the curves represent variations from three experiments for each sample design. The Young's modulus (proportional to stiffness), strength (maximum stress), and toughness (area underneath stress-strain curve) values are compared in Fig. 3(c) and (d) for 80 % and 70 % volume fractions, respectively. It can be seen that the aperiodic monotile-based structures show higher modulus and strength compared to the honeycomb or square-tile structures for both volume fraction cases. The aperiodic monotile structures exhibit superiority in toughness compared to other designs except for rotated square-tile structures, but the high toughness of rotated square-tile structures is due to the high fracture strain (even with low modulus). The high fracture strain of the rotated square-tile structures is most likely due to the low stress concentration at the notch tip delaying crack initiation. With an 80 % volume fraction of VeroClear material, the aperiodic structures (AP80_T1, AP80_T2, and AP80_R1) are approximately 130 % superior in modulus, 65.2 % in strength, and 31.6 % in toughness on average compared to the honeycomb structure (HC80). Crack paths for aperiodic monotile (AP70_R1) and rotated honeycomb structures (HC70_R1) over time are compared in Fig. 4. Crack paths for the other designs can be found in Fig. S2 (See Supplementary Information). The honeycomb or square-tile structure exhibits a path reminiscent of brittle fracture, whereas the aperiodic monotile-based structures reveal a multifaceted crack trajectory with a combination of large and small zigzags, enhancing crack resistance. These results indicate that the aperiodic monotile-based composites have not only higher stiffness, but also higher strength and toughness compared to the honeycomb or square-

Please cite this article in press as: J. Jung et al., Materials Today (2024), https://doi.org/10.1016/j.mattod.2023.12.015

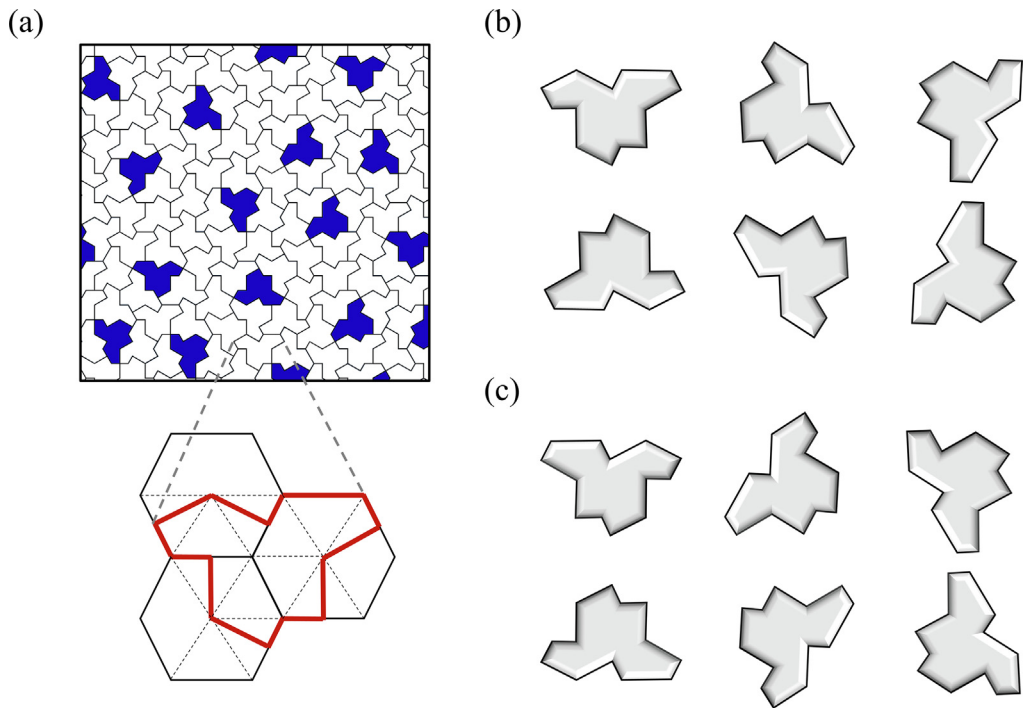

FIG. 1

(a) Tiling schematic of a hat (polykite) aperiodic monotile. Hat monotiles can have (b) six rotational angles and (c) a flipped shape of them. The flipped tiles are presented as dark blue color in (a).

tile structures showing the mechanical superiority of the aperiodic structure, which can be advantageous in many applications. Thanks to the nature of aperiodicity, the aperiodic monotile structures also show consistent stress–strain curves regardless of pattern rotation which implies nearly isotropic characteristics while other structures show some anisotropy. This characteristic has also been shown in various aperiodic structures in the literature [28–30].

To probe further into the mechanisms, simulations utilizing phase-field modeling are performed for the aperiodic monotile-based design and the other designs. More details about the phase-field model are discussed in the Methods section. The simulations are carried out on 2D specimens, each measuring 50 mm by 75 mm (without gripping section) and featuring a notch with 20 % length of the sample, under the tensile loading. The simulations have utilized material properties obtained from the characterization of the base materials (See Table S1 and Fig. S3 in Supplementary Information). In our phase-field model, we have assumed a perfectly bonded interface. This assumption is based on the premise that stress concentration near the crack tip will be a dominant factor in the failure mechanism. Additionally, we have observed in our experimental tests on aperiodic monotile-based composites that the TangoBlackPlus phase remains on both sides of the fracture surface, as shown in Fig. S2 and Fig. S4 (See Supplementary Information). This suggests that failure occurs within the TangoBlackPlus phase, rather than at the interface with VeroClear, supporting our initial assumption of a perfectly bonded interface. Interfacial debonding can be modeled with a cohesive zone model [31,32] combined with a phase-field model if the interfacial bonding becomes comparable to inner phase fracture. The stress–strain curves obtained from simulations for the various designs are shown in Fig. 5, with the general trends matching the experimental results. Here, the aperiodic monotile-based structures show higher modulus, strength, and toughness compared to the honeycomb or square-tile structures. Additionally, it can be seen that the aperiodic monotile-based structures show relatively consistent mechanical performance (similar to experiments) regardless of the crack location or direction determined by the translation or rotation of the tiling. This points to the potential defect tolerance capabilities of these types of aperiodic structures.

The crack propagation behavior of the aperiodic monotile specimen (AP80_T2 in Fig. 5(a)) with different strains can be found in Fig. 6(a, c). The crack propagation behavior of the honeycomb structure with different strains can be found in Fig. 6(b, d). In this model, a phase value of 1 symbolizes complete damage (represented by the color red), while a phase value of 0 denotes no damage (represented by the color blue). Elements exhibiting more than 98 % damage are not depicted. In the phase-field model, as the strain increases, the phase value of the element under stress increases, which indicates the degree of damage and crack propagation. From Fig. 6(a, c), the aperiodic monotile structures show a complex crack path mixed with large and small zigzags, a behavior that is also seen in experiments. Conversely, the crack path in the honeycomb specimen pursued the shortest possible trajectory as shown in Fig. 6(b, d). Crack paths for various designs from phase-field modeling are shown in Fig. S5 (See Supplementary Information), showing that aperiodic monotile structures have a more complex crack path. For a quantitative analysis, the length of the crack path and number of turning during crack propagation for each design are shown in Fig. S6 (See Supplementary Information). We note that there are slight differ-

Please cite this article in press as: J. Jung et al., Materials Today (2024), https://doi.org/10.1016/j.mattod.2023.12.015

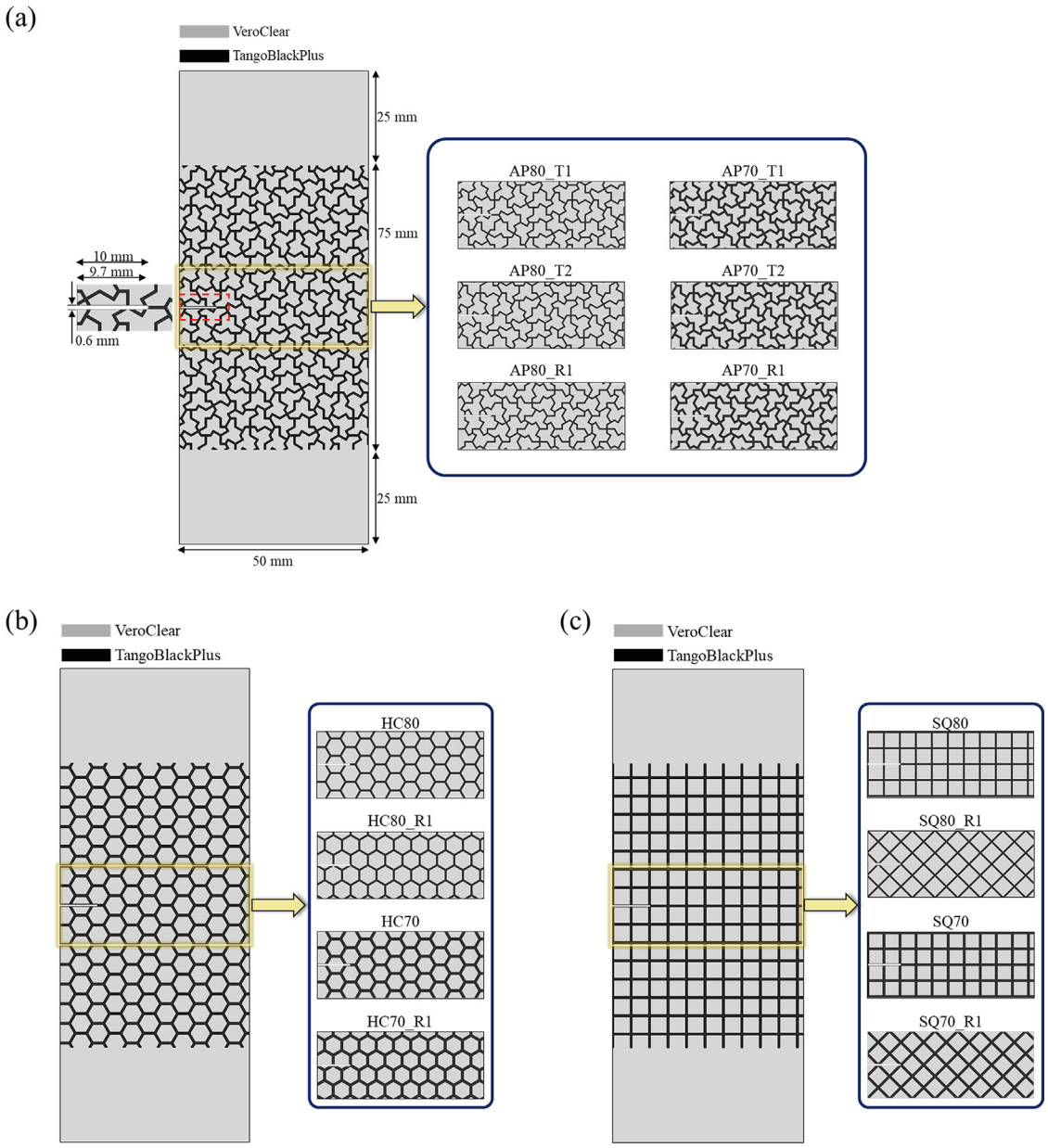

FIG. 2

Specimen schematics for aperiodic monotile, honeycomb, and square-tile composite structures. (a) Designs of aperiodic monotile-based structures with different locations, angles, and volume fractions (80 % and 70 % volume fractions of VeroClear material) are presented. Designs of (b) honeycomb and (c) square-tile structures with different volume fractions (80 % and 70 % volume fractions of VeroClear material) are presented. The thickness of the specimens is 3 mm.

ences between crack paths between simulation and experiments. This may be due to the anisotropic nature of the 3D printing materials themselves which is considered to be isotropic in simulations, as well as the possibility of fractures brought on by microdefects produced during the manufacturing process. Nevertheless, phase-field modeling based simulations are effective for identifying trends of mechanical performance for various composite designs. These results indicate that phase-field modeling holds the potential for capturing the fracture behaviors of these unique composite systems, hence offering promise for future exploration.

The fracture behaviors of aperiodic monotile and honeycomb structures with different notch lengths are further investigated in Fig. S7 (See Supplementary Information), which shows modulus, strength, and toughness decrease with increasing notch length. In this study, TangoBlackPlus is used for boundaries, and VeroClear is used for cores to explore the structural advantage of the aperiodic monotile-based composite. If the material properties of the two phases are comparable or the material combination is switched (VeroClear as boundaries and TangoBlackPlus as cores) or exchanged, the crack would penetrate the cores and interfaces as shown in Fig. S8 (See Supplementary Informa-

Please cite this article in press as: J. Jung et al., Materials Today (2024), https://doi.org/10.1016/j.mattod.2023.12.015

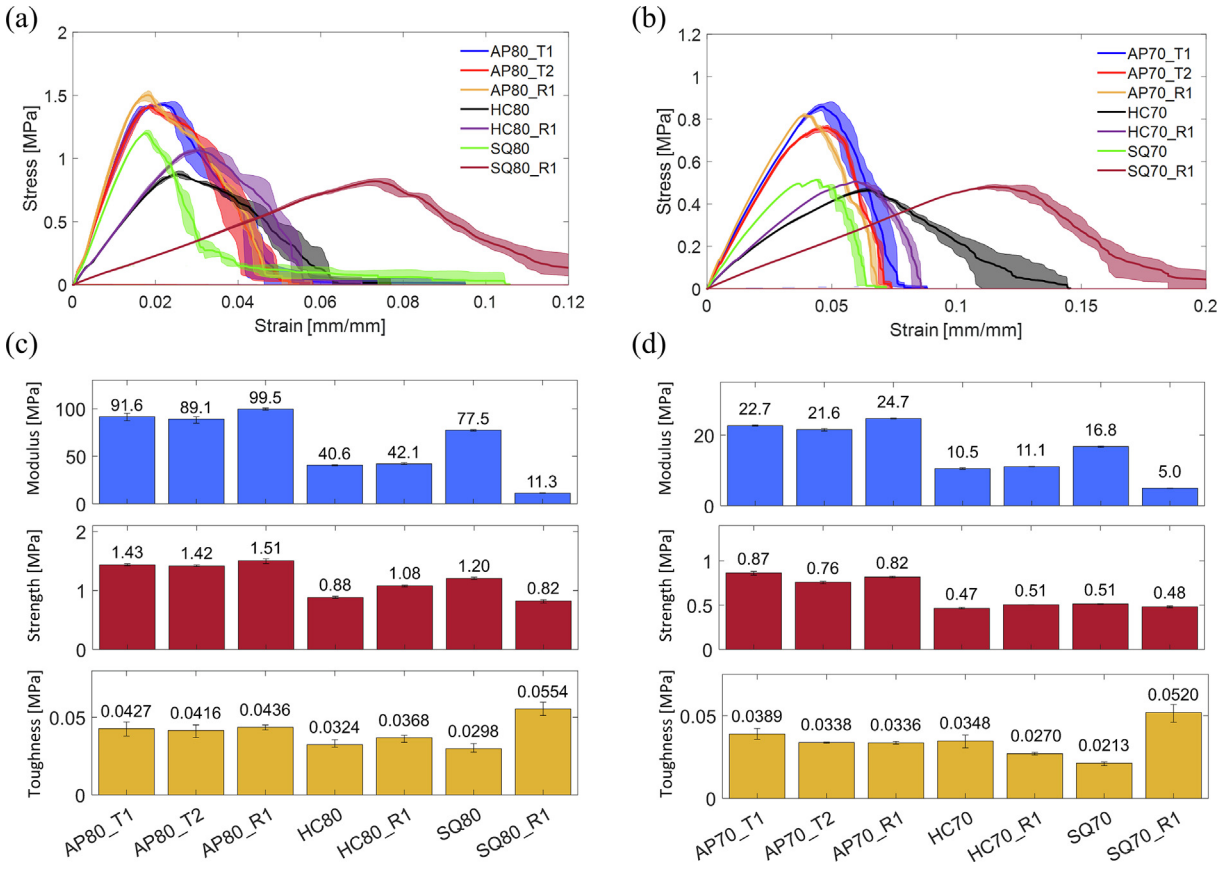

FIG. 3

Experimental results for aperiodic monotile (AP), honeycomb (HC), and square-tile (SQ) structures for (a) 80% and (b) 70% volume fractions of VeroClear material. Solid lines represent the mean value of the three repeated experiments, and the variation is presented as a shaded area. Comparison of Young's modulus, strength, and toughness values of the various structures for volume fractions of (c) 80% and (d) 70%.

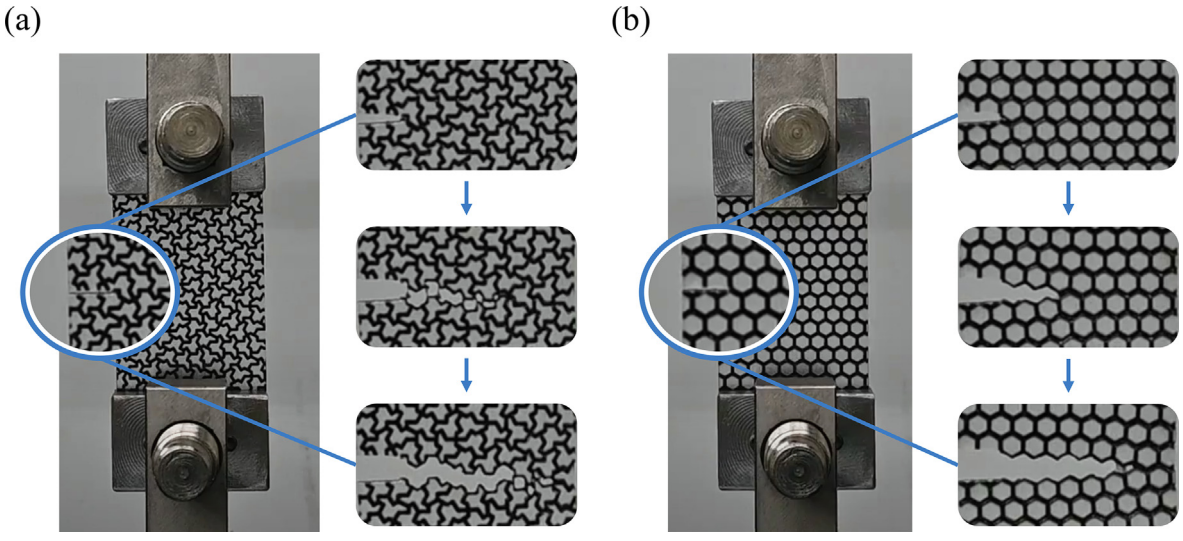

FIG. 4

Snapshots from the experiments under tensile loading for (a) aperiodic monotile (AP70_R1) and (b) rotated honeycomb (HC70_R1) structures. The snapshots of crack initiations (top) and crack propagation (middle and bottom) are presented on the right.

tion), which requires a comprehensive consideration of the interrelationship among fracture strengths of each phase and interfacial bonding. Representative bioinspired structures oftentimes have pronounced anisotropy [33–36] or intricate structures which can be challenging to model using a unit cell. However, this 'hat' aperiodic monotile composite enables not only nearly

Please cite this article in press as: J. Jung et al., Materials Today (2024), https://doi.org/10.1016/j.mattod.2023.12.015

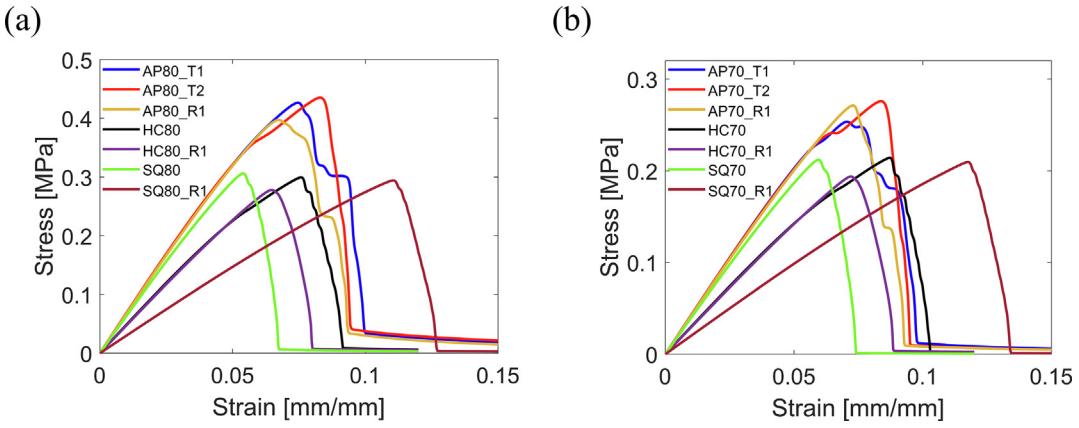

FIG. 5

Finite element analysis results using phase-field model for aperiodic monotile (AP), honeycomb (HC), and square-tile (SQ) structures with (a) 80% and (b) 70% volume fractions of VeroClear material. For aperiodic monotile-based structures, two translated specimens (T1 and T2) and one rotated specimen (R1) are examined, and the honeycomb and square-tile structures are considered as a benchmark comparison.

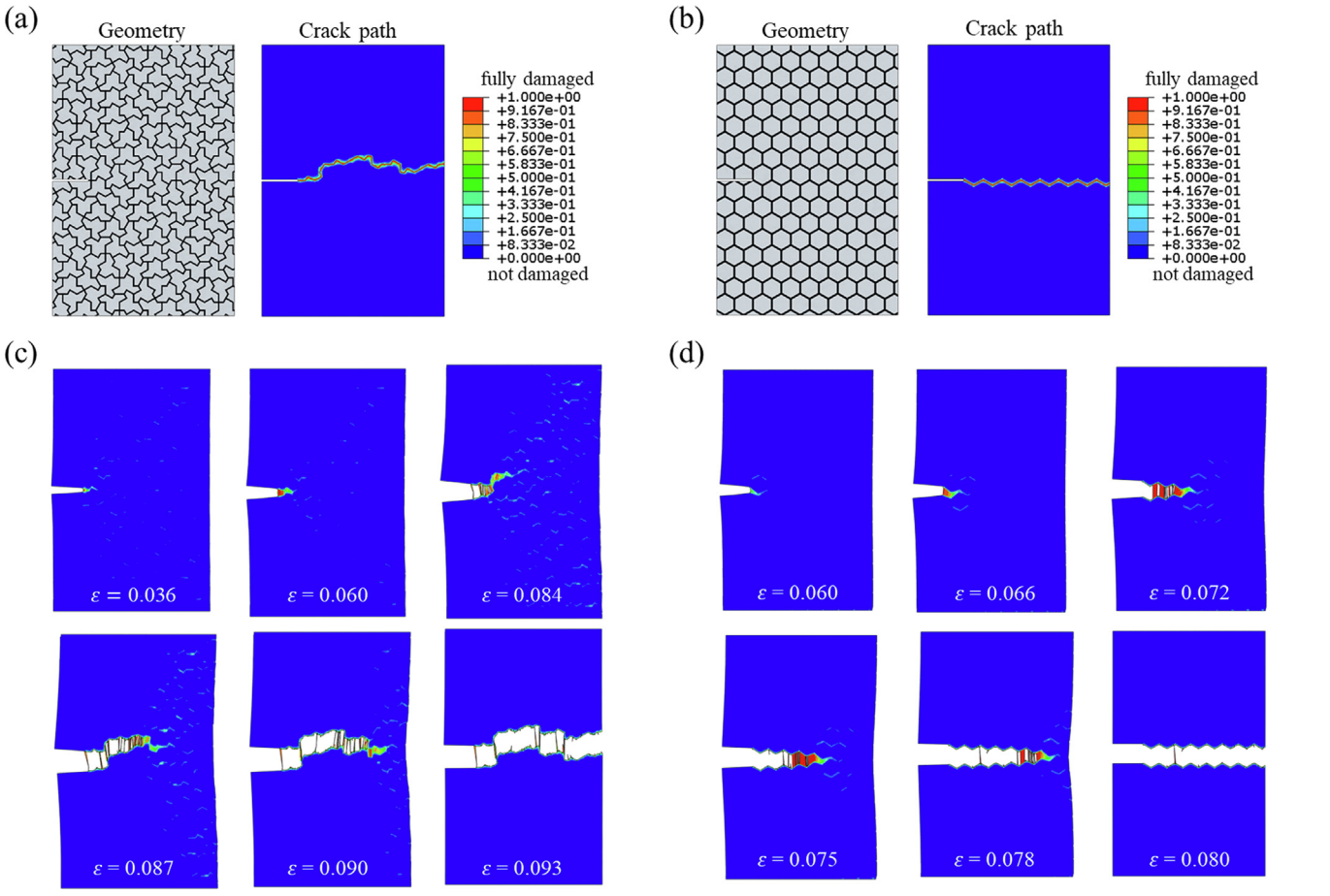

FIG. 6

Comparison results from the phase-field model for aperiodic monotile design (AP80_T2) and honeycomb structure (HC80). (a, b) Geometry and undeformed crack propagation results of the specimen are presented. Crack propagation behavior with strain (ε) increments (scale factor = 1) for (c) the aperiodic monotile structure and (d) the honeycomb structure, respectively. Elements with over 98 % damage are not shown.

isotropic behavior with a single shape of tiles but also superior mechanical performance. An interesting line of future work would be incorporating the effects of anisotropic material properties, unit cell size, and process parameters including printing direction into the simulation. In addition, various aperiodic monotile shapes, such as the 'turtle' or 'Spectre' tile [37], have been discovered after the initial discovery of the 'hat' monotile, and it would be interesting to explore the mechanical behavior

Please cite this article in press as: J. Jung et al., Materials Today (2024), https://doi.org/10.1016/j.mattod.2023.12.015

of composite structures with different aperiodic monotile shapes. We envision that the proposed aperiodic monotile composite structures can be applied to various fields that require high crack resistance under complex loads, such as aerospace, automotive, construction, or energy industries. The structures can be applied not only in a way covering a flat or curved surface but also in a wrapping manner forming a cylindrical shape or in a layer-by-layer laminated form.

Conclusions

This study introduced new architectures incorporating aperiodic monotiles into composite designs. Aperiodic monotile structures greatly simplify composite design because the infinite plane can be covered with a single shape while maintaining aperiodicity. From a manufacturing perspective, the structure provides a wider range of choices in the manufacturing process because the whole structure can be created all at once, or multiple unit tiles can be produced and assembled by simply rotating or flipping the tiles. Furthermore, their aperiodicity offers a promising path to enhanced mechanical resilience while maintaining consistent characteristics regardless of structure orientation. Tensile experiments and corresponding numerical phase-field models show that these aperiodic monotile designs outperform traditional honeycomb-based or square-tile designs in terms of stiffness, strength, and toughness. Furthermore, our findings highlighted the aperiodic designs' inherent capability to tolerate defects with various crack locations and directions. It will be interesting to investigate the effects of aperiodic monotile shapes, unit cell size, volume fraction, wall thickness, and material selection on aperiodic monotile composites in future studies. Through the synthesis of aperiodic materials design, advanced manufacturing techniques, and numerical simulations, this research illuminates a promising avenue for the next generation of composite materials.

Methods

Mechanical testing

Experimental tensile tests (Mode I fracture) on aperiodic monotile, honeycomb, and square-tile structures are conducted. To secure the specimens, mechanical vise action grips are utilized, clamping only the designated gripping area made of the Vero-Clear material. The tests are conducted at a controlled tensile displacement rate of 2 mm/min. Throughout the tests, force, displacement, and time data are recorded at a frequency of 1.04 Hz. The test terminates when the force is dropped to nearly zero, and the crack fully propagated through the transverse direction of the specimen. At least three specimens are printed and tested for each microstructure.

Phase-field modeling

Phase-field modeling is employed due to its established capabilities in simulating intricate crack evolution phenomena including curvilinear crack paths and crack branching [38–40]. Among various versions of phase-field modeling including isotropic formulation, anisotropic formulation, and hybrid formulation, we adopt a hybrid formulation-based phase modeling that can be applicable for combined shear and tensile loading (See Note 1 in Supplementary Information) [41]. The isotropic formulation is only valid for Mode-I fracture because cracks propagate in both tension and compression in the formulation. In contrast, the anisotropic formulation only degrades stiffness in the direction orthogonal to the crack path, causing unrealistic load bearing in the other direction even in fully damaged regions [42]. The hybrid formulation combines strain energy degradation of the anisotropic formulation and stiffness degradation of the isotropic formulation to overcome these drawbacks [43], which enables modeling crack propagation for composites with complex microstructures. The phase-field modeling is conducted using ABAQUS with a user-defined element (UEL) subroutine. The model consisted of three layers including the phase-field layer, displacement layer, and visualization layer sharing the identical nodes. For the simulation, material properties as shown in Table S1 are used for each material. Young's modulus and Poisson's ratio define elastic behavior, the critical energy release rate is equal to the energy creating fracture surface per unit area where strength will increase with the critical energy release rate, and the regularization parameter determines the width of the diffusive crack topology [41]. Approximately 150,000 quadrilateral plane stress elements are used for each layer of specimens. The y-directional displacement of the lower surface is fixed, and the displacement control is applied to the upper surface.

CRediT authorship contribution statement

Jiyoung Jung: Formal analysis, Methodology, Writing – original draft, Investigation. **Ailin Chen:** Formal analysis, Methodology, Writing – original draft, Investigation. **Grace X. Gu:** Conceptualization, Formal analysis, Methodology, Writing – original draft.

Declaration of competing interest

The authors declare that they have no known competing financial interests or personal relationships that could have appeared to influence the work reported in this paper.

Acknowledgements

This research was supported by Office of Naval Research (Fund Number: N00014-21-1-2604), Army Research Office (Fund Number: W911NF-22-1-0175), and National Science Foundation Supercomputing Resources (Fund Number: ACI-1548562).

Appendix A. Supplementary material

Supplementary data to this article can be found online at https://doi.org/10.1016/j.mattod.2023.12.015.

References

[1] B.G. Compton, J.A. Lewis, Adv. Mater. 26 (34) (2014) 5930.
[2] D. Park et al., Mater. Des. 223 (2022) 111192.
[3] X. Wang et al., Compos. Part B: Eng. 110 (2017) 442.
[4] S. Lee et al., Cell Rep. Phys. Sci. (2022) 101152.
[5] Y.-Y. Tsai et al., ACS Biomater. Sci. Eng. (2021).
[6] M.A. Meyers et al., Prog. Mater Sci. 53 (1) (2008) 1.
[7] G.X. Gu et al., Adv. Mater. 29 (28) (2017) 1700060.
[8] S.E. Naleway et al., Adv. Mater. 27 (37) (2015) 5455.
[9] M.K. Habibi et al., Mech. Mater. 97 (2016) 184.
[10] G.X. Gu et al., J. Mech. Behav. Biomed. Mater. 76 (2017) 135.
[11] M.E. Launey et al., Annu. Rev. Mat. Res. 40 (2010) 25.
[12] R.A. Metzler et al., Adv. Funct. Mater. 29 (5) (2019) 1805734.

Please cite this article in press as: J. Jung et al., Materials Today (2024), https://doi.org/10.1016/j.mattod.2023.12.015

[13] K. Liu et al., Science 377 (6609) (2022) 975.
[14] Y. Xu et al., Mater. Des. 162 (2019) 143.
[15] L. Mizzi et al., Smart Mater. Struct. 27 (10) (2018) 105016.
[16] Y. Chiang et al., Compos. Struct. 262 (2021) 113349.
[17] O. Al-Ketan, Metals 11 (2021) 10.
[18] A. Ajdari et al., Int. J. Solids Struct. 48 (3) (2011) 506.
[19] S. Raghavendra et al., Fatigue Fract. Eng. Mater. Struct. 44 (5) (2021) 1178.
[20] T. Mukhopadhyay, S. Adhikari, Int. J. Solids Struct. 91 (2016) 169.
[21] W. Chen et al., Acta Mater. 73 (2014) 259.
[22] M.-S. Pham et al., Nature 565 (7739) (2019) 305.
[23] C. Liu et al., Nat. Commun. 12 (1) (2021) 4600.
[24] M. Kadic et al., Phys. Rev. Appl 2 (5) (2014) 054007.
[25] W.-Y. Jang, S. Kyriakides, Int. J. Solids Struct. 46 (3) (2009) 617.
[26] D. Smith, et al., arXiv preprint arXiv:2303.10798 (2023)
[27] L. Zhang et al., Int. J. Mech. Mater. Des. 16 (2020) 155.
[28] C. Imediegwu et al., Mater. Des. 229 (2023) 111922.
[29] D.J. Clarke et al., Appl. Mater. Today 35 (2023) 101959.
[30] C. Imediegwu et al., J. Strain Anal. Eng. Des. (2023) 03093247221150666.
[31] D.-W. Kim et al., Compos. B Eng. 225 (2021) 109314.
[32] M. Elices et al., Eng. Fract. Mech. 69 (2) (2002) 137.
[33] C. Zhang et al., Adv. Mater. 28 (30) (2016) 6292.
[34] X. Wang et al., Adv. Funct. Mater. 31 (20) (2021) 2010068.
[35] Z. Liu et al., Adv. Funct. Mater. 30 (10) (2020) 1908121.
[36] X. Lu et al., Carbohydr. Polym. (2023) 120669.
[37] D. Smith et al., arXiv preprint arXiv:2305.17743 (2023)
[38] J.-Y. Wu et al., Adv. Appl. Mech. 53 (2020) 1.
[39] D. Schneider et al., Comput. Methods Appl. Mech. Eng. 312 (2016) 186.
[40] J. Choo et al., Acta Geotech. (2023) 1.
[41] H. Jeong et al., Comput. Mater. Sci 155 (2018) 483.
[42] C. Miehe et al., Comput. Methods Appl. Mech. Eng. 199 (45–48) (2010) 2765.
[43] M. Ambati et al., Comput. Mech. 55 (2015) 383.

Please cite this article in press as: J. Jung et al., Materials Today (2024), https://doi.org/10.1016/j.mattod.2023.12.015